On variability of the radiative characteristics in the 940-nm band at variations of water vapor in the atmosphere: numerically simulated results

T.B. Zhuravleva and K.M. Firsov

Institute of Atmospheric Optics,
Siberian Branch of the Russian Academy of Sciences, Tomsk

We consider relationships of solar radiation transfer in the water vapor absorption band at 940 nm in cloud-free atmosphere and in the presence of broken clouds (for summer conditions of Novosibirsk). It is shown that the calculations with underestimated (overestimated) values of the H_2O content in the atmosphere lead to errors in calculated fluxes of downward radiation. At the center of the absorption band, these errors can reach tens of percent. The neglect of continuum absorption in the 870–1030 nm region leads to overestimation of the atmospheric column absorption by 0.8–1.5 W/m^2 (at the solar zenith angle of 30°), depending on the water vapor content. The spectral fluxes we have calculated ourselves well compare with the data of field measurements obtained at the ARM SGP site during the campaign in 1997–1998.

Introduction

Water vapor is well known to be one of the key atmospheric constituents, which determines the processes of cloud formation and aerosol transformation, transfer of solar and thermal radiation, etc. This requires high-quality measurements of H_2O and its vertical profiles in the atmosphere in different meteorological situations,[1] as well as improved H_2O parameterizations in radiation codes.[2,3]

Barker et al.[4] compared modern radiation codes used for study of solar radiation transfer through the atmosphere and for radiation calculations in different weather and climate models. The comparison has shown that most of the 1D codes based on the solution of deterministic radiative transfer equation underestimate atmospheric absorption of solar radiation relative to the benchmark Code for High-Resolution Accelerated Radiative Transfer (CHARTS). In authors' opinion, to a considerable degree this discrepancy is due to the use of parameterizations based on the outdated spectroscopic databases LOWTRAN7 and HITRAN92, as well as due to neglect of H_2O continuum absorption.

The estimates presented by Barker et al.[4] also show that the 1D codes inadequately describe the radiative properties of realistic 3D cloud fields because of the neglect of horizontal inhomogeneity of clouds and imperfect assumptions of cloud overlap at different atmospheric levels. This stimulates the development of 3D radiative codes, usable both for testing of new methods intended for computing heating (cooling) rates in atmospheric general circulation models, and for obtaining more accurate estimates of spectral fluxes and brightness fields in retrieval of atmospheric characteristics from satellite and ground-based radiation measurements.

Presently there are a few radiation codes which are based on newer database HITRAN96.[5,6] These codes make it possible to calculate radiative characteristics with moderate spectral resolution taking into account 3D cloud effects. Earlier we have presented effective statistical algorithms for calculation of the spectral radiative fluxes in clear sky and cloudy atmosphere, including broken clouds.[7] These algorithms are based on representation of transmission function in terms of the exponential series (k-distribution method) and enable one to perform calculations taking into account the instrumental functions of actual instruments. It was also shown that downward solar fluxes, we calculated ourselves and those measured with Rotating Shadowband Spectroradiometer (RSS),[8] under conditions of horizontally homogeneous clouds in the wavelength range 550–650 nm agree reasonably well.

In this paper we will consider the relationships of solar radiative transfer in H_2O absorption band at 940 nm, and continue previously initiated[7] comparison of calculated and measured spectral fluxes in the cloudy atmosphere, and discuss the sensitivity of radiative characteristics to variations of water vapor content (WVC) in the atmosphere.

1. Downward solar fluxes: simulation and measurement results

As noted in the Introduction, in Ref. 7 we have presented results of comparison of the model-based

and measured solar radiation fluxes under conditions of *horizontally homogeneous overcast* in the spectral interval 550–650 nm. The measurements were performed during 1997–1998 campaign at the Atmospheric Radiation Measurement (ARM) Southern Great Plains (SGP) site, Oklahoma, USA.[9,10] The data on spectral fluxes were obtained with Rotating Shadowband Spectroradiometer (RSS), measuring direct, diffuse, and total radiation in channels 512/1024 within the range from 350 to 1075 nm. These same data will also be used here for comparison of model calculations with the field measurements in the absorption band at 940 nm.

The effective molecular absorption coefficients were calculated for simplified (Gaussian) instrumental functions of RSS (512 channels) (ftp://oink.asrc.cestm.albany.edu pub/RSS102) and spectral solar constant by Kurutz[11] using HITRAN-04 database (http://www.hitran.com) and modern models of the continuum absorption (http://tweb.aer.com/continuum_code.html). Information on the state of the atmosphere and cloud layer, necessary for calculations, has been extensively described in Ref. 7. The optical characteristics of aerosol correspond to the model of continental aerosol.[12]

Figure 1 presents spectral fluxes of downward solar radiation $Q(\lambda)$, measured at the surface with two different RSS and calculated using our algorithm and MOTRAN4 radiation code. (The last calculations were kindly presented to us by Z. Li, A. Trishchenko, and M. Cribb, Canadian Centre for Remote Sensing, Ottawa, Canada.) The measured and numerical results agree quite well, except at the center of the H_2O absorption band at 940 nm. Around the center of the band the minimum calculated $Q(\lambda)$ values are biased with respect to measured $Q_{meas}(\lambda)$ in both codes: on October 19, 1997, the minimum of $Q(\lambda)$ was observed at $\lambda = 935$ nm versus minimum of $Q_{meas}(\lambda)$ at $\lambda \sim 939$ nm; whereas on August 5, 1998, the minimum of $Q(\lambda)$ had shifted leftward and was at $\lambda = 933$ nm in comparison with minimum of $Q_{meas}(\lambda)$ at $\lambda \sim 937–941$ nm. In addition, the calculated $Q(\lambda)$ values are lower than the experimental data by almost a factor of two. We note that the measurements were conducted using two different specimens of the device in different atmospheric situations, with a relatively dry atmosphere in one case (WVC = 1.6 g/cm^2) (Fig. 1a) and in a moist atmosphere in the other one (WVC = 4.1 g/cm^2) (Fig. 1b).

One of the possible causes for such a discrepancy may be imperfection of the used parameterizations of the optical characteristics of liquid-water clouds. Moreover, in the calculations we replaced the instrumental functions of the devices with their simplified (Gaussian) approximations. However, these assumptions can be considered only as hypotheses: more certain answer will await further studies.
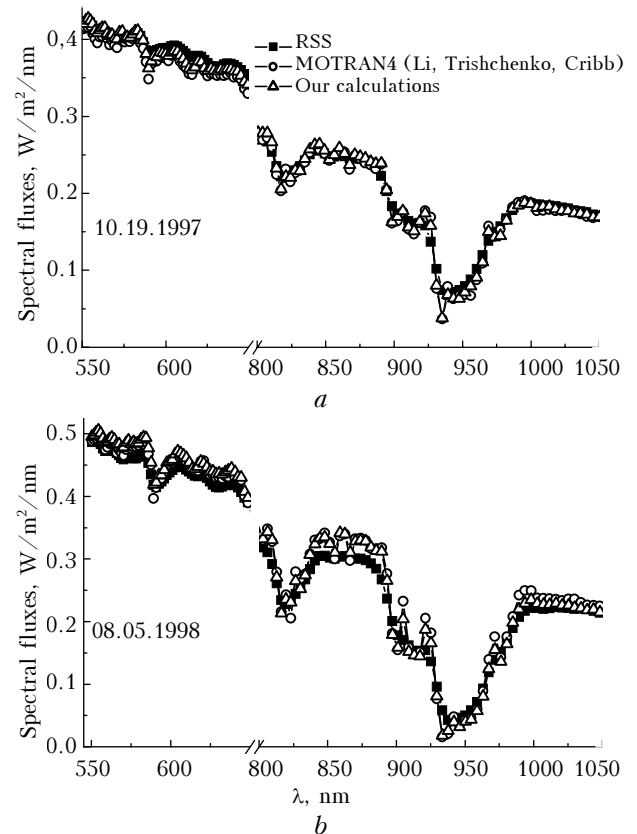

Fig. 1. Downward solar fluxes at the surface level at ARM SGP site and model calculations: liquid water path LWP = 0.008 cm, ozone content is 340 DU; position of the cloud layer: 0.58–0.85 km; effective radius r_{eff} = 7.2 μm; SZA = 47° (a); and LWP = 0.019 cm; ozone content is 330 DU; position of the cloud layer: 1.49–1.88 km; effective radius r_{eff} = 10.8 μm; ZSA = 24° (b).

Note that the algorithm used was previously tested as part of the International Project "Intercomparison of 3D Radiation Codes" (I3RC).[13] It was used to calculate radiative characteristics in complex three-dimensional media (including realistic cloud fields) which well agree with the results of other I3RC project participants. Thus, our radiation code correctly describes both the spectral behavior of solar radiation in the considered wavelength range and the effects caused by spatial 3D cloud structure. Therefore, it can be used to treat solar radiation transfer in the real atmosphere.

2. Influence of variations of water vapor in the atmosphere on radiative characteristics

2.1. Water vapor

To estimate the variations of the spectral radiative characteristics due to variations of water vapor in the atmosphere, we used data of aerological sounding obtained for summer conditions of Novosibirsk (54°N, 83°E) during 1961–1970: profiles

of temperature in the height range from 0 to 30 km, and humidity profiles in the height range from 0 to 7 km. As a rule, the aerological sounding was performed twice a day (00:00 and 16:00 local time), yielding 360 profiles. Profiles of temperature and humidity outside the aforementioned height ranges were added according to the data of meteorological AFGL model.[14] Variations of temperature and water vapor concentration, as well as WVC distribution (g/cm^2) for summer conditions of Novosibirsk are presented in Figs. 2a–c. The average value $\overline{WVC} = 2.6\ g/cm^2$ is close to the average WVC in AFGL model (2.98 g/cm^2), the standard deviation $\sigma_{WVC} = 0.7\ g/cm^2$, and minimum (min)WVC and maximum (max)WVC values are 1.1 and 4.1 g/cm^2, respectively.

Figure 2d shows plot of the ratio of atmospheric transmittance T in two spectral channels, at 870 and 940 nm, of an SP-6 photometer (as described by Sakerin et al.[15]) versus absorbing mass of water vapor mWVC, where m is the atmospheric mass calculated by line-by-line method and according to two-parameter approximation formula as given by Chesnokova et al.[16] It follows from the simulation results that the atmospheric transmittance in this spectral range is a function of mWVC and depends weakly on variations of temperature and air pressure. In this regard, in what follows we restrict ourselves to consideration of 5 vertical H_2O profiles corresponding to the $\overline{WVC}$, $\overline{WVC} \pm \sigma_{WVC}$, as well as minimum and maximum WVC values. Though vertical distribution of water vapor in the atmosphere is intrinsically different in the presence and absence of clouds, we also will use the given profiles in radiation flux calculations under conditions of partial cloud cover (for cloud fractions $N \leq 0.5$).
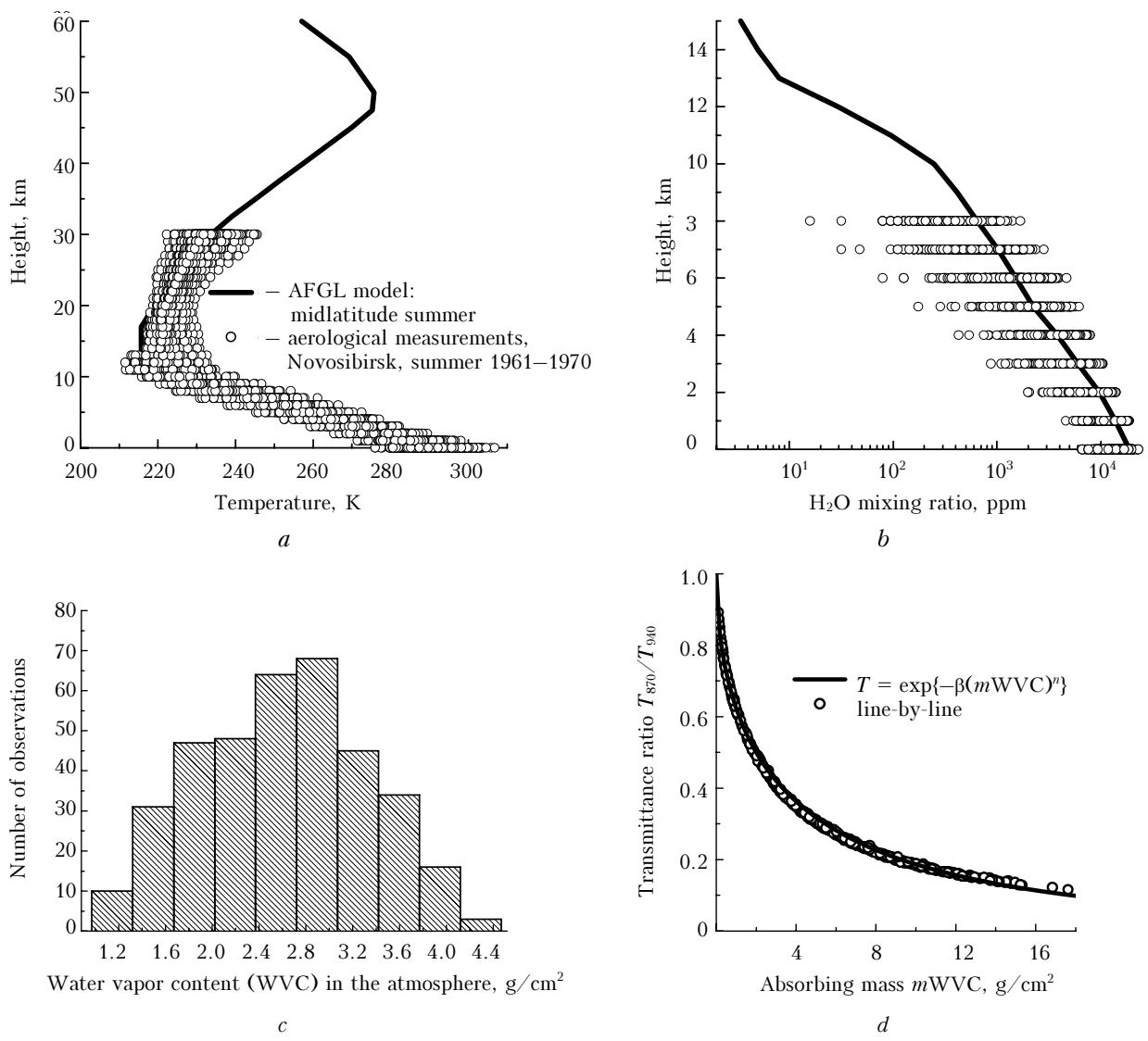

a

b

c

d

Fig. 2

2.2. Radiative characteristics

We will consider the variability of downward fluxes at the surface level and absorption A within the entire atmospheric column in H_2O absorption band at 940 nm. This spectral interval is chosen for its energetic significance: its contribution to fluxes of transmitted (at the surface level) and reflected (at the top of the atmosphere, $H_{atm}^{top} = 100$ km) radiation within the interval 870−1030 nm is ~ 10% for midlatitude summer.[17] Comparative analysis of radiation calculations and measurements in this wavelength range can be used to estimate the quality of water vapor parameterizations in radiation codes. (Recall that, as the single scattering albedo of liquid-water clouds in this spectral interval exceeds 0.999, the absorptivity of the atmosphere is primarily determined by water vapor.) In addition, the spectral measurements of diffuse radiation in H_2O absorption band at 940 nm may be helpful for development of new methods of retrieval of water vapor content in atmospheric column (see, e.g., Ref. 18).

The calculations presented below are performed for the following atmospheric parameters: surface albedo $A_s = 0.2$, position of the cloud layer is 1−2 km, mean horizontal cloud size $D = 1$ km, and cloud extinction coefficient $\sigma(\lambda = 550$ nm$) = 10$ km^{-1}.

Downward radiation

Variations of spectral fluxes of diffuse $Q_s(\lambda)$, not scattered $S(\lambda)$, and total $Q(\lambda) = Q_s(\lambda) + S(\lambda)$ radiation under conditions of WVC varying relative to the mean $\overline{\text{WVC}}$ values will be characterized by the quantity

$$\Delta F(\lambda) = 100\% \cdot \left(F(\text{WVC}, \lambda) - F(\overline{\text{WVC}}, \lambda)\right) / F(\overline{\text{WVC}}, \lambda),$$
$$F = Q, \ Q_s, \ S.$$

Obviously, the error in the total radiation $Q(\lambda)$ will depend not only on $\Delta Q_s(\lambda)$ and $\Delta S(\lambda)$, but also on the contribution from each of these components to $Q(\lambda)$.

Examples of calculations of diffuse $Q_s(\lambda)$ and not scattered $S(\lambda)$ radiation under conditions of clear sky and moderate cloud cover (cloud fraction $N = 0.5$) for different WVC values are presented in Figs. 3a and c: for $N = 0$ not scattered radiation dominates, and as cloud fraction and solar zenith angle (SZA) increase the main contributor to $Q(\lambda)$ turns out to be the diffuse component.

When H_2O content varies in the atmosphere, maximum variations of $Q_s(\lambda)$ and $S(\lambda)$ and, hence, $Q(\lambda)$ take place near center of the absorption band at 940 nm. In the absence of clouds, for SZA = 30°, a decrease/increase of water vapor content by approximately 30% (variation coefficient $v = 100\% \cdot \dfrac{\sigma_{\text{WVC}}}{\overline{\text{WVC}}} \approx 30\%$) leads to a mutually comparable changes in the spectral fluxes (Table 1):

$$|\Delta Q(\lambda, \overline{\text{WVC}} - \sigma_{\text{WVC}})| \approx |\Delta Q(\lambda, \overline{\text{WVC}} + \sigma_{\text{WVC}})|.$$

As SZA increases, $|\Delta S(\lambda)|$ and, hence, $|\Delta Q(\lambda)|$ become asymmetric:

$$|\Delta Q(\lambda, \overline{\text{WVC}} - \sigma_{\text{WVC}})| > |\Delta Q(\lambda, \overline{\text{WVC}} + \sigma_{\text{WVC}})|.$$

Table 1. Relative variations of downward spectral fluxes $\Delta Q(\lambda)(\%)$ for different water vapor contents in the atmosphere at the center of the absorption band at 940 nm. The cloud-free atmosphere

Absorption band, nm	SZA = 30°				SZA = 75°			
	WVC, g/cm²							
	1.1	1.9	3.3	4.1	1.1	1.9	3.3	4.1
929.42	33	11	−13	−21	79	24	−24	−36
933.56	90	28	−27	−40	272	71	−48	−66
937.72	77	26	−23	−34	190	55	−40	−56
941.9	56	21	−20	−31	163	50	−40	−56

This asymmetry increases as WVC further deviates from $\overline{\text{WVC}}$: with the decrease of WVC by ~ 60% (which corresponds to minWVC = 1.1 g/cm²), $|\Delta Q(\lambda)|$ exceeds $|\Delta Q(\lambda)|$ corresponding to maxWVC = = 4.1 g/cm² by more than a factor of three. As follows from the calculated results, far from the center of the absorption band this effect still exists: if $|\Delta Q(\lambda)|$ is considered as a function of WVC, its maximum is shifted toward minWVC (Figs. 3b and d).

Qualitatively similar situation is observed under conditions of partial cloud cover (Fig. 3d).

The radiation measurements used for comparison with model calculations generally have temporal resolutions of a few minutes at most. It is also well known that the frequency of aerological sensing can vary from once every 3 h during intensive observation periods to once every 6−12 h in periods of routine measurements. Since water vapor content in the atmosphere can vary within wide range during a day (Fig. 4), a question may arise: to what errors in radiation calculation the deficiency of our knowledge about WVC can lead?

Suppose that all atmospheric parameters with the exception for water vapor are accurately specified, and instead of "true" values $\text{WVC}^* = \overline{\text{WVC}} \mp \sigma_{\text{WVC}}$ we will use average value $\overline{\text{WVC}}$ in the calculations. Let us determine the calculation error of downward radiation as follows:

$$\text{Er}Q(\lambda) = 100\% \times$$
$$\times \left(Q(\overline{\text{WVC}}, \lambda) - Q(\text{WVC}^*, \lambda)\right) / Q(\text{WVC}^*, \lambda).$$

It can be easily found that $\text{Er}Q(\lambda)$ is related to $\Delta Q(\lambda)$ by the formula

$$\text{Er}Q(\lambda) = \frac{-100\% \cdot \Delta Q(\lambda)}{100\% + \Delta Q(\lambda)}.$$

According to data from Table 1 the use of overestimated (2.6 instead of 1.9 g/cm²) WVC values near absorption band center leads to underestimation of $Q(\lambda)$ by 20−40%, depending on SZA. When $Q(\lambda)$ is calculated using underestimated WVC values (2.6 instead of 3.3 g/cm²), $\text{Er}Q(\lambda)$ increases up to ~ 30−70%.
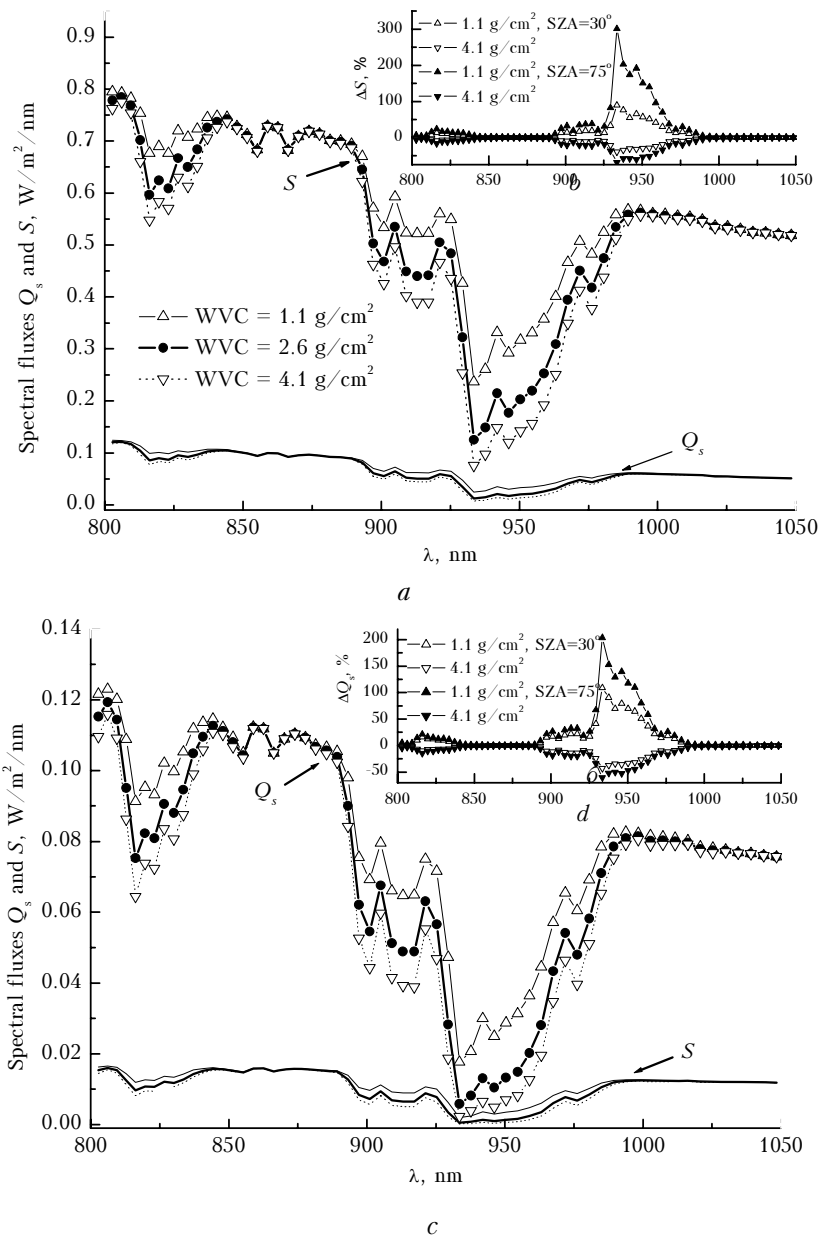
a

c

Fig. 3. Spectral fluxes of diffuse $Q_s(\lambda)$ and not scattered $S(\lambda)$ radiation and their variations due to variations of the WVC: clear sky, SZA = 30° (*a*); broken clouds, $N = 0.5$, SZA = 75° (*b*).

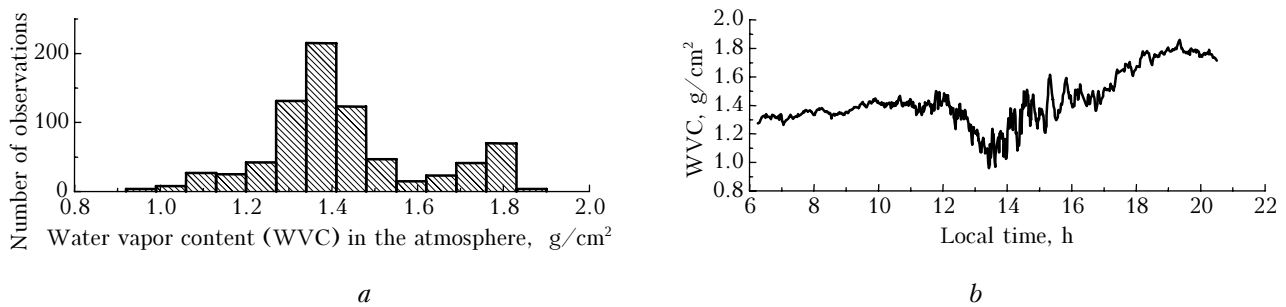*a*   *b*

Fig. 4. Variations of water vapor in the atmosphere during a day. Water vapor content in the atmosphere is retrieved using an original method[16] based on the measurement data of SP-4 sun photometer (Tomsk, IAO SB RAS) and spectroscopic database HITRAN-04.

Absorption in the atmosphere

Within the spectral interval from 870 to 1030 nm, we shall consider the integrated absorption by the atmosphere A and its absorptance

$$\text{Abs} = 100\% \cdot A / Q(z = H_{\text{atm}}^{\text{top}}),$$

where

$$Q(z = H_{\text{atm}}^{\text{top}}) = \int\limits_{870\,\text{nm}}^{1030\,\text{nm}} Q(\lambda, z = H_{\text{atm}}^{\text{top}}) \mathrm{d}\lambda$$

is the integrated flux of solar radiation incident on the top of the atmosphere.

The dependence of A and Abs (%) in the absence of clouds and in the presence of broken clouds on WVC is shown in Table 2.

Atmospheric absorption is the sum of absorption in above-cloud (A^{up}) and below-cloud (A^{down}) atmosphere, as well as within the cloud layer (A^{cl}). For fixed SZA and a given H_2O profile, an increase in the cloud fraction N leads to an increase in albedo of the cloud layer and, hence, to the growth of absorption of the above-cloud atmosphere. The larger N, the greater the number of photon collisions with cloud matter, favoring the growth of A^{cl}. At the same time, the fractions of radiation coming to the cloud layer and below-cloud atmosphere decrease accordingly. This leads to the fact that A^{cl} and A^{down} (for moderate surface albedos A_s) have a tendency toward a decrease.

Depending on cloud properties (height of cloud top, cloud optical depth, and cloud fraction N), water vapor content in the atmosphere, and observation conditions (A_s and SZA), each of the above-mentioned factors influences the atmospheric absorption A to a larger or smaller degree. When SZA changes in the range of SZA $\leq 60°$, occurrence of low-level clouds leads, as a rule, to an increase in the absorption[19]: $A_{\text{clr}} \leq A_{\text{low}}$. Difference between A_{clr} and A_{low} increases with growing N and WVC in the atmosphere. As solar zenith angle increases to ~75°, the albedo of clouds increases and absorption within the cloud layer can decrease. The difference between A_{clr} and A_{low} is reduced, and situations are possible when the occurrence of low-level clouds may lead to a decrease in the absorption by H_2O in the atmosphere. It is just this situation that we observe for the considered parameters of the atmosphere.

Contribution of H₂O continuum absorption

It is recognized that, in order to reconcile simulation and measurement results, radiation codes must account for continuum absorption by water vapor. For instance, Tarasova and Fomin[20] showed that the contribution of water vapor continuum absorption in the intervals of 700−1220 nm and 1220−2270 nm is 3 W/m² and 4.6 W/m², respectively, and that the total effect in the entire near-infrared region is 10 W/m² (midlatitude summer, SZA = 30°).

From our calculations it follows that for SZA=30° the contribution of continuum absorption in the considered interval of 870−1030 nm varies approximately from 0.8 to 1.5 W/m² as WVC increases from minimum to maximum value (1.1−4.1 g/cm²). For SZA = 75° the continuum absorption is ~ 0.3−0.5 W/m². The presented estimates are valid both under clear-sky conditions and in the presence of stochastic clouds (cloud fraction $N \leq 0.5$). We note that the neglect of continuum absorption in the 940-nm band influences more significantly the atmospheric absorption in comparison with the effects of random cloud geometry (in the framework of Poisson model of the broken clouds), which do not exceed 0.3−0.4 W/m² for the above input parameters. (Accuracy of absorption calculation does not exceed 2%).

Conclusion

We have compared model calculations with the results on spectral fluxes of downward radiation measured with RSS under conditions of horizontally homogeneous overcast. Quite good agreement between the results of numerical simulation and experimental data indicates that our algorithm[7] adequately treats the spectral variations of radiation not only under conditions of weak molecular absorption (550−650 nm), but also under conditions of moderate absorption by water vapor (in the range from 800 to 1050 nm).

To study variations of radiative characteristics under conditions of varying of H_2O content in the atmosphere, we used data of aerological sounding, obtained in summer period of Novosibirsk for 10 years. It is shown that near the center of the absorption band, with increase (decrease) of WVC between the limits determined by variation coefficient $v \approx 30\%$ for small solar zenith angles (SZA = 30°) $|\Delta Q(\lambda)|$ is symmetrical and equals ~ 30%.

Table 2. Absorption A (W/m²) and absorptance of the atmosphere Abs (in parentheses, %)
in the wavelength range from 870 to 1030 nm under clear sky conditions and in broken clouds

WVC, g/cm²	Clear sky		Broken clouds			
			N = 0.3		N = 0.5	
	SZA = 30°	SZA = 75°	SZA = 30°	SZA = 75°	SZA = 30°	SZA = 75°
1.1	22.3 (19.8)	11.1 (32.8)	22.4 (19.8)	9.3 (27.7)	23.1 (20.5)	8.9 (26.5)
2.6	31.3 (27.8)	14.0 (41.4)	31.6 (28.0)	12.4 (36.7)	32.4 (28.7)	12.0 (35.6)
4.1	36.7 (32.5)	15.6 (46.3)	37.1 (32.9)	14.2 (42.0)	37.9 (33.6)	13.8 (40.9)

Further change of H_2O content in the atmosphere and growth of SZA leads to the asymmetry of $|\Delta Q(\lambda)|$: maximum $|\Delta Q(\lambda)|$ values, exceeding 100%, are shifted toward minimum WVC values. As a consequence the errors in $\Delta Q(\lambda)$ calculation appear due to overestimated (underestimated) WVC values used in calculations, which may reach few tens of percent in the center of the absorption band.

It is also shown that the neglect of continuum absorption by water vapor in the band from 870 to 1030 nm can lead to underestimation of the absorption A: at SZA = 30° this value is 0.8–1.5 W/m^2, depending on H_2O content in the atmosphere.

The obtained estimates must be kept in mind in comparing data of numerical simulations with the data of field measurements.

Acknowledgments

References

1. H.E. Revercomb, D.D. Turner, D.C. Tobin, R.O. Knuteson, W.F. Feltz, J. Barnard, J. Bosenberg, S. Clough, D. Cook, R. Ferrare, J. Goldsmith, S. Gutman, R. Halthore, B. Lesht, J. Liljegren, H. Linne, J. Michalsky, V. Morris, W. Porch, S. Richardson, B. Schmid, M. Splitt, T. Van Hove, E. Westwater, and D. Whiteman, Bull. Amer. Meteorol. Soc. **84**, No. 2, 217–236 (2003).
2. R. Ellingson, J. Ellis, and S. Fels, J. Geophys. Res. D **96**, No. 5, 8929–8954 (1991).
3. Y. Fouquart, B. Bonnel, and V. Ramaswamy, J. Geophys. Res. D **96**, No. 5, 8955–8968 (1991).
4. H. Barker, G.L. Stephens, P.T. Partain, J.W. Bergman, B. Bonnel, K. Kampana, E.E. Clothiaux, S. Clough, S. Cusack, J. Delamere, J. Edwards, K.F. Evans, Y. Fouquart, S. Freidenreich, V. Galin, Y. Hou, S. Kato, J. Li, E. Mlawer, J.–J. Morcrette, W. O'Hirok, P. Raisanen, V. Ramaswamy, B. Ritter, E. Rozanov, M. Schlesinger, K. Shibata, P. Sporyshev, Z. Sun, M. Wendisch, N. Wood, and F. Yang, J. Climate **16**, No. 16, 2676–2699 (2003).
5. W. O'Hirok and C. Gautier, J. Atmos. Sci. **55**, No. 12, 2162–2179 (1998).

6. T.C. Benner and K.F. Evans, J. Geophys. Res. D **106**, No. 14, 14975–14984 (2001).
7. T.B. Zhuravleva and K.M. Firsov, Atmos. Oceanic Opt. **17**, No. 11, 799–806 (2004).
8. L. Harrison, J. Berndt, P. Kiedron, J. Michalsky, Q. Min, and J. Schlemmer, in: *Proceedings of the Ninth Atmosph. Rad. Measur. (ARM) Science Team Meeting.* Available URL: http://www.arm.gov/docs/documents/technical/conf_9903/harrison–99.pdf.
9. Z. Li, A. Trishchenko, and M. Cribb, in: *Proc. of the Tenth Atmosph. Rad. Measurem. (ARM) Science Team Meeting.* Available URL: http://www.arm.gov/publications/proceedings/conf10/abstracts/li–z.pdf.
10. Z. Li, M. Cribb, and A. Trishchenko, in: *Proc. of the Eleventh Atmosph. Rad. Measurem. (ARM) Science Team Meeting.* Available URL: http://www.arm.gov/publications/proceedings/conf11/abstracts/li–z.pdf.
11. T.L. Kurucz, in: *IAU Symp. 154,* ed. by D.M. Rabin and J.T. Jefferies (Kluwer, Acad. Norwell Massachusetts, 1992).
12. *A preliminary cloudless standard atmosphere for radiation computation. World Climate Research Programme.* WCP–112, WMO/TD, No. 24 (1986), 60 pp.
13. R. Cahalan, L. Oreopoulos, A. Marshak, K.F. Evans, A. Davis, R. Pincus, K. Yetzer, B. Mayer, R. Davies, T. Ackerman, H. Barker, E. Clothiaux, R. Ellingson, M. Garay, E. Kassianov, S. Kinne, A. Macke, W. O'Hirok, P. Partain, S. Prigarin, A. Rublev, G. Stephens, E. Takara, T. Varnai, G. Wen, and T. Zhuravleva, Bull. Amer. Meteorol. Soc. (2005) (in press).
14. G. Anderson, S. Clough, F. Kneizys, J. Chetwynd, and E. Shettle, *AFGL Atmospheric Constituent Profiles (0 – 120 km),* Air Force Geophysics Laboratory. AFGL–TR–86–0110. Environ. Res. Paper No. 954 (1986).
15. S.M. Sakerin, D.M. Kabanov, A.P. Rostov, S.A. Turchinovich, and Yu.S. Turchinovich, Atmos. Oceanic Opt. **17**, No. 4, 314–320 (2004).
16. T.Yu. Chesnokova, K.M. Firsov, D.M. Kabanov, and S.M. Sakerin, Atmos. Oceanic Opt. **17**, No. 11, 807–810 (2004).
17. V. Ramaswamy and S.M. Freidenreich, J. Geophys. Res. D **96**, No. 5, 9133–9157 (2004).
18. P. Kiedron, J. Berndt, L. Harrison, J. Michalsky, and Q. Min, in: *Proc. of the 11th Atmosph. Rad. Measurem. (ARM) Science Team Meeting:* http://www.arm.gov/publications/ proceedings/conf11/abstracts /kiedron1–pw.pdf.
19. T.B. Zhuravleva, Atmos. Oceanic Opt. **11**, No. 8, 730–736 (1998).
20. T. Tarasova and B. Fomin, J. Appl. Meteorol. **39**, No. 11, 1947–1951 (2000).